

# CHEMISTRY

## A European Journal

A Journal of



### Accepted Article

**Title:** Ni<sub>3</sub> vs Ni<sub>30</sub>. A Truncated Octahedron Metal-Organic Cage Constructed with [Ni<sub>5</sub>(CN)<sub>4</sub>]<sup>6+</sup> Squares and Tripodal Tris-tacn Ligands that are Large and Flexible

**Authors:** Zongyao Zhang, Kunyi Zheng, Tianlong Xia, Lijin Xu, and Rui Cao

This manuscript has been accepted after peer review and appears as an Accepted Article online prior to editing, proofing, and formal publication of the final Version of Record (VoR). This work is currently citable by using the Digital Object Identifier (DOI) given below. The VoR will be published online in Early View as soon as possible and may be different to this Accepted Article as a result of editing. Readers should obtain the VoR from the journal website shown below when it is published to ensure accuracy of information. The authors are responsible for the content of this Accepted Article.

**To be cited as:** *Chem. Eur. J.* 10.1002/chem.201604598

**Link to VoR:** <http://dx.doi.org/10.1002/chem.201604598>

Supported by  
**ACES**

WILEY-VCH

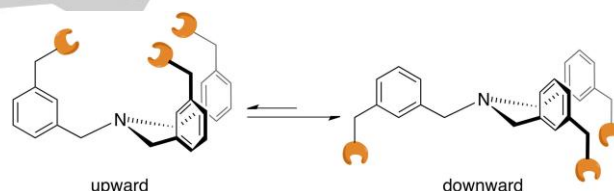
# Ni<sub>3</sub> vs Ni<sub>30</sub>. A Truncated Octahedron Metal-Organic Cage Constructed with [Ni<sub>5</sub>(CN)<sub>4</sub>]<sup>6+</sup> Squares and Tripodal Tris-tacn Ligands that are Large and Flexible\*\*

Zongyao Zhang, Kunyi Zheng, Tianlong Xia, Lijin Xu, and Rui Cao\*

**Abstract:** Reactions of trinickel complex of tripodal tris-tacn ligand N(CH<sub>2</sub>-*m*-C<sub>6</sub>H<sub>4</sub>-CH<sub>2</sub>tacn)<sub>3</sub> (**L**, tacn = 1,4,7-triazacyclononane) in acetonitrile-methanol solution with and without phosphate led to two complexes of distinct nuclearities, [(Ni<sup>II</sup>Cl)<sub>3</sub>(CH<sub>3</sub>OH)<sub>3</sub>(HPO<sub>4</sub>)<sub>3</sub>]**L**(PF<sub>6</sub>) (Ni<sub>3</sub>, **1**) and [(Ni<sup>II</sup><sub>5</sub>(CN)<sub>4</sub>(H<sub>2</sub>O)<sub>8</sub>Cl)<sub>6</sub>]**L**<sub>3</sub>Cl<sub>30</sub> (Ni<sub>30</sub>, **2**). Ligand **L** takes upward and downward conformation in the structure of **1** and **2**, respectively. It is proposed that phosphate directs the upward conformation of Ni<sub>3</sub>**L** to form **1**. In the absence of phosphate, Ni<sub>3</sub>**L** assembles with cyanide ions, which are formed via Ni-catalyzed C–CN bond cleavage of acetonitrile, to give nano-sized Ni<sub>30</sub> cage. Complex **2** represents a discrete truncated octahedron cage assembled with [Ni<sub>5</sub>(CN)<sub>4</sub>]<sup>6+</sup> squares and large and flexible triangular ligands, which is scarcely observed for self-assembled metal-organic cages. Magnetic properties of **1** and **2** were examined, showing intriguing magnetic properties.

Self-assembled metal-organic coordination cages have attracted extensive research interests because of their intrinsic structural features and their potential applications in host-guest chemistry and material science.<sup>[1–12]</sup> The construction of metal-organic cages is realized by the self-assembly of metal ions or metal clusters typically occupying the vertexes of a discrete polyhedron and organic ligands linking them as either the edges or the faces of the polyhedron. Recent efforts have resulted in a variety of coordination cages with single metal ions,<sup>[13–18]</sup> M<sub>2</sub>,<sup>[19–21]</sup> and M<sub>4</sub><sup>[22–25]</sup> metal clusters acting as vertexes, but cages with vertexes of higher nuclearity metal clusters are very rare. On the other hand, rigid linear/bent or facial ligands with preorganized binding angles are usually required for the assembly of cages because ligands of flexible conformation and binding ability generally result in mixed coordination species.<sup>[6]</sup> Therefore, molecular metal-organic cages using building blocks of high-nuclearity metal clusters as vertexes and flexible ligands as linkages are scarcely reported in the literature.

Recently, Cao and Lippard designed a series of multidentate tripodal ligands using the tribenzylamine scaffold functionalizing either its ortho or meta position with different ligand appendages.<sup>[26–29]</sup> The resulted trinuclear metal complexes have been shown to be able to capture biologically relevant μ<sub>3</sub>-oxoanions, such as phosphate and carbonate, and effectively catalyze the hydrolysis of phosphate esters. In the course of exploring this ligand system, we found that such tris(xylyl) linker arms are highly flexible, and ligands functionalizing at the meta positions have various conformations. For example, Scheme 1 displays the two conformers of tripodal tris-tacn ligand N(CH<sub>2</sub>-*m*-C<sub>6</sub>H<sub>4</sub>-CH<sub>2</sub>tacn)<sub>3</sub> (**L**, tacn = 1,4,7-triazacyclononane) with three arms pointing to either upward or downward direction. The upward conformer was observed in μ<sub>3</sub>-oxoanion-directed assembly of M<sub>3</sub>**L** (M = Mn, Cu, or Zn),<sup>[26]</sup> but attempts to structurally determine the downward conformer of **L** and its metal complexes were unsuccessful largely due to the high flexibility of the ligand.



**Scheme 1.** Schematic representation showing the upward and downward conformations of ligand **L**. The downward conformer is thermodynamically more favored due to the less steric hindrance between three bulky ligand arms

Herein we reported the synthesis and X-ray structures of two nickel complexes of **L** with distinct nuclearities. Reactions of **L** and NiCl<sub>2</sub> in acetonitrile-methanol solutions with and without phosphate led to Ni<sub>3</sub> complex **1** and Ni<sub>30</sub> complex **2**, respectively (Scheme 2). Similar to our previous results, phosphate directs the upward conformation of Ni<sub>3</sub>**L** to give **1**. Unexpectedly, in the absence of phosphate, a nano-sized Ni<sub>30</sub> cage **2** was formed through the assembly of downward Ni<sub>3</sub>**L** with *in situ* generated cyanide ions. The truncated octahedron cage of **2** is unique as it is constructed with pentanuclear [Ni<sub>5</sub>(CN)<sub>4</sub>]<sup>6+</sup> squares and large and flexible ligand **L** triangles. Magnetic properties of **1** and **2** were also examined, showing intriguing magnetic properties.

Reaction of three equivalents of NiCl<sub>2</sub> with one equiv. of **L** in an acetonitrile-methanol mixture gave a clear light green solution at room temperature. After addition of one equiv. of Na<sub>2</sub>HPO<sub>4</sub> and stirring the mixture at 60 °C for 6 h, an excess amount of solid NH<sub>4</sub>PF<sub>6</sub> was added. Slow evaporation of the resulted solution led to the isolation of green crystals of **1** in 66% yield. Crystallographic studies revealed that **1** was analogue to the trimetallic complexes we reported previously (Scheme 2 and Figure 1A).<sup>[26]</sup> It crystallizes in the trigonal space group *R*3̄c with *a* = 15.5930(9) Å, *c* = 78.327(9) Å, *V* = 16493(2) Å<sup>3</sup>, and *Z* =

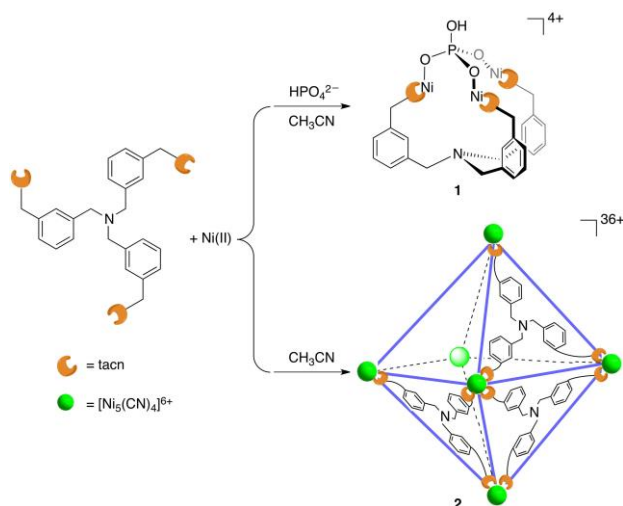
[\*] Z. Y. Zhang, K. Y. Zheng, Prof. Dr. L. J. Xu, Prof. Dr. R. Cao  
Department of Chemistry  
Renmin University of China, Beijing 100872 (China)  
E-mail: [ruicao@ruc.edu.cn](mailto:ruicao@ruc.edu.cn)

Prof. Dr. R. Cao  
School of Chemistry and Chemical Engineering  
Shaanxi Normal University, Xi'an 710119 (China)  
Prof. Dr. T. L. Xia  
Department of Physics  
Renmin University of China, Beijing 100872 (China)

[\*\*] We are grateful for support from the "Thousand Talents Program" of China, the National Natural Science Foundation of China (No. 21101170 and 21573139), the Fundamental Research Funds for the Central Universities, and the Research Funds of Renmin University of China.

Supporting information for this article is available on the WWW under

12.<sup>[30]</sup> The trinickel unit of **1** is located at the special position with a crystallographically required  $C_3$  axis passing through the central N atom (N1) and  $\mu_3$ -phosphate group (P1, O2). The three symmetric tacn-based ligand arms each bind one  $Ni^{II}$  atom through three N atoms. The three Ni atoms are bridged together by a phosphate group with each Ni binding to one of the three facial O atoms, resulting in a  $Ni\cdots Ni$  separation of 5.499 Å. The distorted octahedral coordination sphere of each Ni is filled by a terminal chloride and a methanol group (Figure 1B).



**Scheme 2.** Synthesis of  $Ni_3$  complex **1** and  $Ni_{30}$  complex **2** from the reaction of  $Ni_3L$  with and without phosphate ions in acetonitrile-methanol solutions.

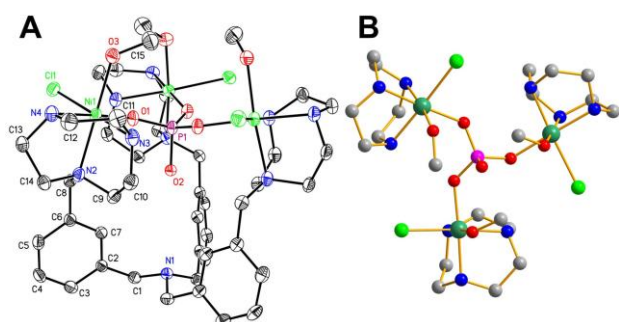


**Figure 1.** (A) Thermal ellipsoid plot (50% probability) of the X-ray structure of **1**. All hydrogen atoms are omitted for clarity. (B) Ball-and-stick representation of the  $[Ni_3(PO_4)]$  coordination environment. Color code: green, nickel; light green, chlorine; grey, carbon; blue, nitrogen; red, oxygen; pink, phosphorus.

In the structure of **1**, the triply bridging phosphate group is disordered over two opposite orientations with 80% pointing into the inner cavity of the molecular backbone and the rest 20% pointing out of the inner cavity as determined by free structural refinement. The fourth, uncoordinated O atom (O2) of phosphate is protonated, which is suggested by long P1–O2 bond distance of 1.599(6) Å as compared to short P1–O1 bond distance of 1.479(3) Å. Bond valence sum (BVS) calculation also suggested that the P1–O2 bond only contributed BVS of 1.01 to this O2 atom. In addition, in the X-ray structure of **1**, one  $PF_6^-$  counterion per trinickel unit was found, further confirming the monoprotonation of O2 atom. The three ligand arms of **L** adopt a upward orientation to capture the  $[Ni_3(HPO_4)]^{4+}$  unit. As we demonstrated previously, the downward conformer is

thermodynamically more stable due the less steric hindrance between the three bulky ligand arms.<sup>[26]</sup> This result is therefore another example illustrating the templating effect of phosphate in the tris(xylyl) trimetallic system.

Significantly, reaction of  $NiCl_2$  and **L** in acetonitrile-methanol solution without the addition of  $Na_2HPO_4$  gave  $Ni_{30}$  complex **2**, whose structure was unexpected (Scheme 2). After heating and stirring the reaction mixture at 60 °C for 6 h, the clear light green solution gradually turned to purple. During slow evaporation, this solution became more intensely purple colored, and finally led to the isolation of violet crystalline prisms of **2** in 3 weeks with a moderate yield (see Supporting Information for details).

Crystallographic studies revealed that complex **2** crystallized in the tetragonal space group  $I4$  with  $a = 32.4457(15)$  Å,  $c = 29.6336(13)$  Å,  $V = 31196(2)$  Å<sup>3</sup>, and  $Z = 2$ .<sup>[30]</sup> The discrete coordination cage of **2** consists of 30 Ni atoms, 24 cyanide ions, 8 tris-tacn ligand **L**, 6 chloride ions, and 48 aqua groups, which together afford a nano-sized molecular cage of 30 Å in diameter (Figure 2A). This  $Ni_{30}$  cage is located at a special position with the crystallographically required  $C_4$  axis passing through the Cl1–Ni6–Ni9–Cl1 axis, and it can be in principle viewed as a truncated octahedron<sup>[31,32]</sup> with six  $[Ni_5(CN)_4]^{6+}$  squares occupying the vertexes and eight tripodal **L** ligands linking them as the faces of the octahedron (Figure 2B and 2D). For each  $[Ni_5(CN)_4]^{6+}$  square four Ni atoms reside at the four corners of a square planar, and they are bridged together through a  $\mu_4$ - $Ni(CN)_4$  unit (Figure 2C). For  $\mu_2$ - $\eta^1, \eta^1$ -groups linking the central and corner Ni atoms, we assigned them as cyanide ions based on (1) they are two-atom units with a linear bridging mode and (2) the bond lengths of 1.154(13) Å (by average) between the two atoms are very short. All these results are consistent with triply-bonded groups. As it is not likely to form  $C\equiv C$  groups under the synthetic conditions, we assigned them as cyanide ions, which could be generated *in situ* via Ni-catalyzed C–CN bond cleavage of acetonitrile. Such bond activations have been investigated in detail by Jones and co-workers experimentally and theoretically, who demonstrated that Ni complexes were able to catalyze the C–CN bond cleavage of various organic nitrile complexes.<sup>[33–35]</sup>

The central Ni atom is coordinated by four cyanide ions via the C atoms and is bound to an additional axial chloride ligand, giving a square pyramidal geometry. The average Ni–C distance is 1.858(12) Å, and the average Ni–Cl distance is 2.856(15) Å. Based on comparison of this Ni–C distance to many others reported in  $[Ni(CN)_4]^{2-}$  units,<sup>[36]</sup> this Ni atom has a  $d^8$   $Ni^{II}$  electronic structure. The average C–Ni–C bond angle of 89.78° shows that the Ni atom is located almost perfectly at the center of the square planar. For the four corner Ni atoms, each is coordinated by a tacn moiety of the ligand arm through three N atoms, and is bound to the N atom of the bridging cyanide group. The octahedral coordination geometry of these corner Ni atoms is filled by two additional aqua ligands. BVS calculation of 2.29 suggests  $d^8$   $Ni^{II}$  electronic structures for these corner Ni atoms. Two points are worth noting. First, the average Ni–O bond length of 2.102(11) Å (with the range of 2.038(11) to 2.128(8) Å) is consistent with terminal aqua ligands instead of terminal hydroxyl ligands, as Ni–OH bond lengths are typically smaller than 1.90 Å.<sup>[37]</sup> The Ni–O bond is calculated to contribute BVS of only 0.28–0.35 to these O atoms. Second, the shorter Ni–CN distance of 1.858(12) Å and the longer Ni–NC distance of



2.048(13) Å further confirm the X-ray structure assignment that the bridging cyanide ions bind to the central and corner Ni atoms via C and N atoms, respectively.<sup>[36]</sup>

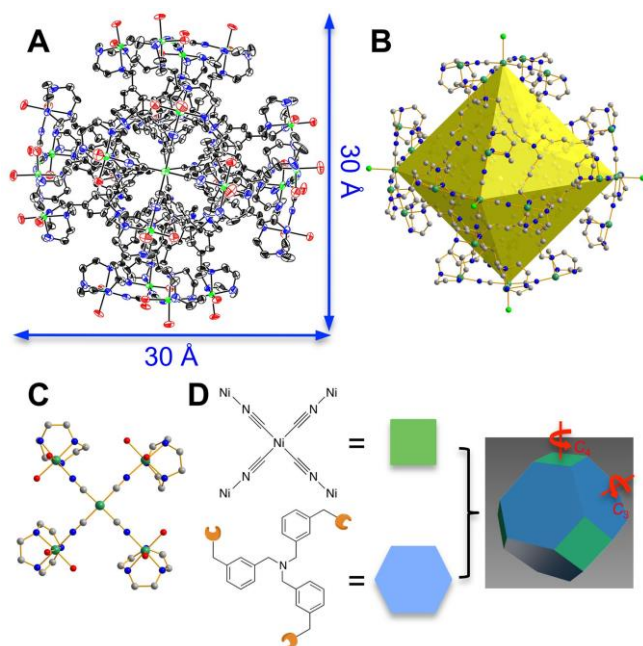


**Figure 2.** (A) Thermal ellipsoid plot (50% probability) of the X-ray structure of **2**. All hydrogen atoms and chloride ions are omitted for clarity. (B) Schematic representation of the molecular structure of **2** with an octahedron geometry. (C) Ball-and-stick illustration of the  $[\text{Ni}_5(\text{CN})_4]^{6+}$  coordination environment. (D) The assembly of truncated octahedron by  $[\text{Ni}_5(\text{CN})_4]^{6+}$  squares and **L** ligands. Color code: green, nickel; light green, chlorine; grey, carbon; blue, nitrogen; red, oxygen.

In  $[\text{Ni}_5(\text{CN})_4]^{6+}$  squares, the average Ni(corner)⋯Ni(central) separation is 5.046 Å, and the average Ni(corner)⋯Ni(corner) separation is 7.066 Å. In the X-ray structure of **2**, 36 chloride ions were found. Six of them bind to the six central Ni atoms, and the rest are found as counter ions in the crystal lattice. Based on crystallographic studies, molecular formula of **2** can be unambiguously determined to be  $[(\text{Ni}^{\text{II}})_5(\text{CN})_4(\text{H}_2\text{O})_3\text{Cl}_6\text{L}_3]\text{Cl}_{30}$ . In addition, a number of co-crystallized solvent water molecules were also found in the X-ray structure. Interestingly, molecules of **2** form one-dimensional chains in X-ray crystal structure along the *c* axis through intermolecular Ni6–Cl1–Ni9 interactions with Ni6–Cl1 bond distance of 2.903(6) Å and Ni9–Cl1 bond distance of 2.928(6) Å (Figure S4). In addition, unlike **1**, the tris-tacn ligand **L** in **2** adopts the downward conformation. This relatively more spread geometry makes the three Ni atoms bound to the same ligand **L** to have Ni⋯Ni separation about 15 Å, which is much larger than the Ni⋯Ni separation of 5.499 Å as observed in the structure of **1**. It is necessary to note that no chloride ions and/or solvent water molecules are found in the inner cavity of **2**, although it is positively charged and its outside diameter is about 30 Å. We rationalize that the inner cavity of **2** has only a small size of  $5.4 \times 5.4 \times 5.4 \text{ Å}^3$ , which is likely due to the bulky ligand **L**.

Although  $[\text{Ni}_5(\text{CN})_4]^{6+}$  units have been reported in literature,<sup>[36]</sup> to the best of our knowledge, complex **2** represents the first example bearing such  $[\text{Ni}_5(\text{CN})_4]^{6+}$  squares as vertexes of cage-like coordination polyhedrons. Possible explanation is

that  $\text{Ni}^{\text{II}}$  ions have strong binding affinity with cyanide ions. As a result, Ni-cyanide species with extended structures are easily formed, which are highly challenging to be isolated and crystallized. The use of multidentate capping ligands, such as tacn, is considered to prevent the growth of extended structures and thus is beneficial for the isolation of complex **2** in our experiments. On the other hand, we also tried to synthesize complex **2** starting from  $\text{NiCl}_2$ , ligand **L** and  $\text{K}_2[\text{Ni}(\text{CN})_4]$ . However, precipitates immediately appeared upon mixing with  $\text{K}_2[\text{Ni}(\text{CN})_4]$ , which is consistent with the formation of insoluble Ni-cyanide species with extended structures (i.e.  $-\text{Ni}-\text{C}\equiv\text{N}-\text{Ni}-\text{N}\equiv\text{C}-\text{Ni}-$ ). We rationalized that during the synthesis of **2** under our experimental conditions, cyanide ions were gradually generated *in situ* through Ni-catalyzed C–CN bond cleavage of acetonitrile.<sup>[33–35]</sup> The generation of cyanide ions and their assembly with  $\text{Ni}^{\text{II}}$  ions and **L** ligands to form **2** are concomitant, which prevents the accumulation of cyanide ions in the reaction mixture. It is therefore considered to be another reason for the successful isolation of **2**. Third,  $[\text{Ni}_5(\text{CN})_4]^{6+}$  unit has a 4-fold rotational symmetry, while tripodal ligand **L** has a 3-fold rotational symmetry. The combination of these two symmetry elements is essential for the formation of truncated octahedron cages (Figure 2D). It is necessary to note that ligand **L** is large and flexible, and is in principle not favored to be used for the self-assembly of coordination metal-organic cages. Therefore, symmetry-directed assembly is also a possible reason for the formation of **2**. Although complex **2** was obtained unexpectedly, it is unique to represent a discrete truncated octahedron cage having  $[\text{Ni}_5(\text{CN})_4]^{6+}$  squares as vertexes and large and flexible tripodal **L** ligands linking them as the faces of the polyhedron.

It is interesting to compare the synthesis and structure of **1** and **2**. The only difference in the synthesis of **1** and **2** is the presence or absence of phosphate ions. As we demonstrated previously, ligand **L** has various conformations with upward and downward conformers depicted in Scheme 1.<sup>[26]</sup> The templating effect of phosphate directed the formation of **1**, which resembles several trimetallic complexes of **L** we reported before. The large binding constant of  $\text{HPO}_4^{2-}$  with  $\text{Ni}_3\text{L}$ , which was determined to be  $3.15 \times 10^5 \text{ M}^{-1}$  (Figure S3), was the possible driving force for **L** to adopt thermodynamically less favorable upward conformation. In the absence of phosphate, **L** takes downward conformation, and  $\text{Ni}_3\text{L}$  assembles with *in situ* generated cyanide ions to give **2**. In our work, the mild reaction conditions, compared with high-pressure, high-temperature solvothermal conditions, has also brought new examples for building up large metal-organic cages.

Transition metal-cyanide clusters have recently attracted particular research interests due to their magnetic properties.<sup>[38–41]</sup> We therefore investigated the magnetism of complexes **1** and **2**. The temperature dependence of magnetic susceptibility of **1** and **2** were measured in 2.5–300 K with an applied field of 100 Oe. The  $\chi_{\text{M}}T$  value of **1** at 300 K is about  $3.6 \text{ cm}^3 \text{ mol}^{-1} \text{ K}$ , which is larger than the spin only value of three isolated  $\text{Ni}^{\text{II}}$  ions with  $S = 1$  ( $3.0 \text{ cm}^3 \text{ mol}^{-1} \text{ K}$ ). As shown in Figure 3A, the susceptibility exhibits a monotonic rise in  $\chi_{\text{M}}T$  with decreasing temperature, suggesting the ferromagnetic coupling between  $\text{Ni}^{\text{II}}$  ions. At low temperature,  $\chi_{\text{M}}T$  value approaches  $4.1 \text{ cm}^3 \text{ mol}^{-1} \text{ K}$ , which is slightly higher than the theoretical value of  $3.9 \text{ cm}^3 \text{ mol}^{-1} \text{ K}$  for an  $S = 3$  ground state of  $\text{Ni}^{\text{II}}$  ( $^3\text{F}_4$ ,  $g = 5/4$ ). The  $\chi_{\text{M}}T$  value of **2** at

300 K is about  $20.0 \text{ cm}^3 \text{ mol}^{-1} \text{ K}$  (Figure 3B), which is much smaller than the spin only values of 30 isolated  $\text{Ni}^{\text{II}}$  ions with  $S = 1$  ( $30.0 \text{ cm}^3 \text{ mol}^{-1} \text{ K}$ ). As we know, the degeneracy of Landau levels of the central  $\text{Ni}^{\text{II}}$  ions will be lifted within square planar crystal field, which results in the central  $\text{Ni}^{\text{II}}$  ions with effective  $S = 0$ . As a result, the number of  $\text{Ni}^{\text{II}}$  ions contributing magnetic moment is 24, instead of 30 as intuitively thought. The curve between 50 and 300 K is well described by Curie-Weiss law with Curie constant  $C = 19.7 \text{ cm}^3 \text{ mol}^{-1} \text{ K}$ , which is obtained by linear fit of temperature dependent  $\chi_{\text{M}}^{-1}$ . The value of the Weiss temperature near zero and the curvature of  $\chi_{\text{M}}T$  clearly indicate the paramagnetism of **2**. When temperature decreases,  $\chi_{\text{M}}T$  approaches  $13.5 \text{ cm}^3 \text{ mol}^{-1} \text{ K}$ , which may be attributed to the zero field splitting.

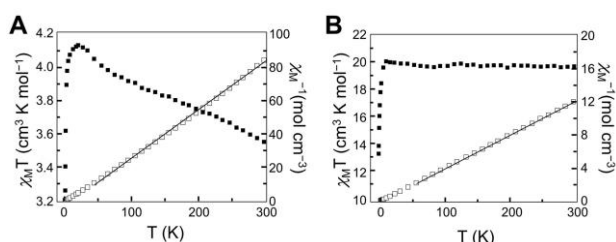


**Figure 3.** Plots of temperature dependence of  $\chi_{\text{M}}T$  and  $\chi_{\text{M}}^{-1}$  for complexes **1** (A) and **2** (B).

In conclusion, we reported two nickel complexes of distinct nuclearities with the use of tripodal tris-tacn ligand **L**. The  $\text{Ni}_3$  complex **1** resembles the trimetallic complexes we reported recently, in which a biologically relevant  $[\text{M}_3(\text{PO}_4)]$  core is kept within the backbone of **L**. The  $\text{Ni}_{30}$  complex **2** can be viewed as a nano-sized cage of truncated octahedron with six  $[\text{Ni}_5(\text{CN})_4]^{6+}$  squares occupying the vertexes and eight **L** ligands linking them as the faces of the octahedron. Various conformations of **L** and the templating effect of phosphate are the origins to form these different products under similar synthetic conditions. Although complex **2** is obtained unexpectedly, it is noteworthy in several aspects, including (1) cyanide ions are generated *in situ* under mild reaction conditions, and the direct use of  $[\text{Ni}(\text{CN})_4]^{2-}$  for the assembly of **2** is unsuccessful; (2) complex **2** represents the first example to have pentanuclear  $\text{M}_5$  building blocks as vertexes and large and flexible ligands as linkages of polyhedrons; (3) symmetry-directed assembly of  $\text{C}_4$ -symmetry  $[\text{Ni}_5(\text{CN})_4]^{6+}$  squares and  $\text{C}_3$ -symmetry **L** ligands is a possible reason for the formation of **2**. Magnetic studies revealed the ferromagnetism of **1** and the paramagnetism of **2**.

**Keywords:** self-assembly • tripodal ligand • nickel • coordination cage • flexible

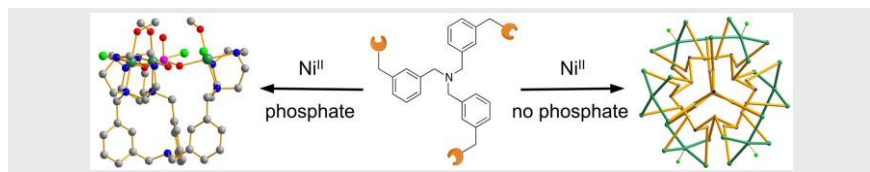
- [1] A. J. McConnell, C. S. Wood, P. P. Neelakandan, J. R. Nitschke, *Chem. Rev.* **2015**, *115*, 7729-7793.
- [2] L. Chen, Q. H. Chen, M. Y. Wu, F. L. Jiang, M. C. Hong, *Acc. Chem. Res.* **2015**, *48*, 201-210.
- [3] A. Galan, P. Ballester, *Chem. Soc. Rev.* **2016**, *45*, 1720-1737.
- [4] M. D. Ward, *Chem. Commun.* **2009**, 4487-4499.
- [5] Y. Fang, T. Murase, S. Sato, M. Fujita, *J. Am. Chem. Soc.* **2013**, *135*, 613-615.

- [6] S. Horiuchi, T. Murase, M. Fujita, *J. Am. Chem. Soc.* **2011**, *133*, 12445-12447.
- [7] N. Rodríguez-Vázquez, M. Amorín, I. Alfonso, J. R. Granja, *Angew. Chem. Int. Ed.* **2016**, *55*, 4504-4508.
- [8] C. Gütz, R. Hovorka, C. Klein, Q. Q. Jiang, C. Bannwarth, M. Engeser, C. Schmuck, W. Assenmacher, W. Mader, F. Topić, K. Rissanen, S. Grimme, A. Lützen, *Angew. Chem. Int. Ed.* **2014**, *53*, 1693-1698.
- [9] R. M. Zhu, J. Lübben, B. Dittrich, G. H. Clever, *Angew. Chem. Int. Ed.* **2015**, *54*, 2796-2800.
- [10] M. Kieffer, B. S. Pilgrim, T. K. Ronson, D. A. Roberts, M. Aleksanyan, J. R. Nitschke, *J. Am. Chem. Soc.* **2016**, *138*, 6813-6821.
- [11] J. Park, L. B. Sun, Y. P. Chen, Z. Perry, H. C. Zhou, *Angew. Chem. Int. Ed.* **2014**, *53*, 5842-5846.
- [12] P. D. Frischmann, V. Kunz, F. Würthner, *Angew. Chem. Int. Ed.* **2015**, *54*, 7285-7289.
- [13] X. P. Zhou, J. Liu, S. Z. Zhan, J. R. Yang, D. Li, K. M. Ng, R. W. Y. Sun, C. M. Che, *J. Am. Chem. Soc.* **2012**, *134*, 8042-8045.
- [14] Y. R. Zheng, W. J. Lan, M. Wang, T. R. Cook, P. J. Stang, *J. Am. Chem. Soc.* **2011**, *133*, 17045-17055.
- [15] D. Fujita, H. Yokoyama, Y. Ueda, S. Sato, M. Fujita, *Angew. Chem. Int. Ed.* **2015**, *54*, 155-158.
- [16] N. Kishi, M. Akita, M. Yoshizawa, *Angew. Chem. Int. Ed.* **2014**, *53*, 3604-3607.
- [17] D. M. Wood, W. J. Meng, T. K. Ronson, A. R. Stefankiewicz, J. K. M. Sanders, J. R. Nitschke, *Angew. Chem. Int. Ed.* **2015**, *54*, 3988-3992.
- [18] W. J. Ramsay, F. T. Szczypiński, H. Weissman, T. K. Ronson, M. M. J. Smulders, B. Rybtchinski, J. R. Nitschke, *Angew. Chem. Int. Ed.* **2015**, *54*, 5636-5640.
- [19] D. Tian, Q. Chen, Y. Li, Y. H. Zhang, Z. Chang, X. H. Bu, *Angew. Chem. Int. Ed.* **2014**, *53*, 837-841.
- [20] M. J. Prakash, M. Oh, X. F. Liu, K. N. Han, G. H. Seong, M. S. Lah, *Chem. Commun.* **2010**, *46*, 2049-2051.
- [21] X. S. Wang, M. Chrzanowski, W. Y. Gao, L. Wojtas, Y. S. Chen, M. J. Zaworotko, S. Q. Ma, *Chem. Sci.* **2012**, *3*, 2823-2827.
- [22] K. C. Xiong, F. L. Jiang, Y. L. Gai, D. Q. Yuan, D. Han, J. Ma, S. Q. Zhang, M. C. Hong, *Chem. Eur. J.* **2012**, *18*, 5536-5540.
- [23] K. C. Xiong, F. L. Jiang, Y. L. Gai, D. Q. Yuan, L. Chen, M. Y. Wu, K. Z. Su, M. C. Hong, *Chem. Sci.* **2012**, *3*, 2321-2325.
- [24] M. Liu, W. P. Liao, C. H. Hu, S. C. Du, H. J. Zhang, *Angew. Chem. Int. Ed.* **2012**, *51*, 1585-1588.
- [25] X. X. Hang, B. Liu, X. F. Zhu, S. T. Wang, H. T. Han, W. P. Liao, Y. L. Liu, C. H. Hu, *J. Am. Chem. Soc.* **2016**, *138*, 2969-2972.
- [26] R. Cao, P. Müller, S. J. Lippard, *J. Am. Chem. Soc.* **2010**, *132*, 17366-17369.
- [27] R. Cao, B. D. McCarthy, S. J. Lippard, *Inorg. Chem.* **2011**, *50*, 9499-9507.
- [28] X. Liu, P. W. Du, R. Cao, *Nat. Commun.* **2013**, *4*, 2375.
- [29] Y. Y. Ning, M. Gao, K. Y. Zheng, Z. Y. Zhang, J. Zhou, X. Hao, R. Cao, *J. Mol. Catal. A: Chem.* **2015**, *403*, 43-51.
- [30] Crystal data for **1**:  $[(\text{Ni}^{\text{II}}\text{Cl})_3(\text{CH}_3\text{OH})_3(\text{HPO}_4)_3\text{L}](\text{PF}_6)_3$ , trigonal,  $R\bar{3}c$ ,  $a = 15.5930(9) \text{ \AA}$ ,  $c = 78.327(9) \text{ \AA}$ ,  $V = 16493(2) \text{ \AA}^3$ ,  $Z = 12$ ,  $T = 153(2) \text{ K}$ , 38917 reflections collected, 3788 unique ( $R_{\text{int}} = 0.0332$ ), final  $R_1 = 0.0606$ ,  $wR_2 = 0.1703$  for 3207 observed reflections [ $I > 2\sigma(I)$ ]. Crystal data for **2**,  $[(\text{Ni}^{\text{II}}_5(\text{CN})_4(\text{H}_2\text{O})_8\text{Cl})_6\text{L}_8]\text{Cl}_{30}$ , tetragonal,  $I4$ ,  $a = 32.4457(15) \text{ \AA}$ ,  $c = 29.6336(13) \text{ \AA}$ ,  $V = 31196(2) \text{ \AA}^3$ ,  $Z = 2$ ,  $T = 150(2) \text{ K}$ , 299083 reflections collected, 32064 unique ( $R_{\text{int}} = 0.0810$ ), final  $R_1 = 0.1069$ ,  $wR_2 = 0.2756$  for 22399 observed reflections [ $I > 2\sigma(I)$ ]. CCDC 1492717 (1) and 1492718 (2) contain the supplementary X-ray data for this paper. These data can be obtained free of charge from the Cambridge Crystallographic Data Centre via [www.ccdc.cam.ac.uk/data\\_request/cif](http://www.ccdc.cam.ac.uk/data_request/cif).
- [31] M. C. Hong, Y. J. Zhao, W. P. Su, R. Cao, M. Fujita, Z. Y. Zhou, A. S. C. Chan, *J. Am. Chem. Soc.* **2000**, *122*, 4819-4820.
- [32] N. Li, F. L. Jiang, L. Chen, X. J. Li, Q. H. Chen, M. C. Hong, *Chem. Commun.* **2011**, *47*, 2327-2329.
- [33] N. M. Brunkan, D. M. Brestensky, W. D. Jones, *J. Am. Chem. Soc.* **2004**, *126*, 3627-3641.

- [34] T. A. Ateşin, T. Li, S. Lachaize, W. W. Brennessel, J. J. García, W. D. Jones, *J. Am. Chem. Soc.* **2007**, *129*, 7562-7569.
- [35] B. D. Swartz, N. M. Reinartz, W. W. Brennessel, J. J. García, W. D. Jones, *J. Am. Chem. Soc.* **2008**, *130*, 8548-8554.
- [36] F. Meyer, R. F. Winter, E. Kaifer, *Inorg. Chem.* **2001**, *40*, 4597-4603.
- [37] D. G. Huang, O. V. Makhlynets, L. L. Tan, S. C. Lee, E. V. Rybak-Akimova, R. H. Holm, *Proc. Natl. Acad. Sci. USA* **2011**, *108*, 1222-1227.
- [38] M. P. Shores, J. J. Sokol, J. R. Long, *J. Am. Chem. Soc.* **2002**, *124*, 2279-2292.
- [39] D. E. Freedman, D. M. Jenkins, A. T. Iavarone, J. R. Long, *J. Am. Chem. Soc.* **2008**, *130*, 2884-2885.
- [40] D. Pinkowicz, H. Southerland, X. Y. Wang, K. R. Dunbar, *J. Am. Chem. Soc.* **2014**, *136*, 9922-9924.
- [41] S. Chorazy, R. Podgajny, K. Nakabayashi, J. Stanek, M. Rams, B. Sieklucka, S. Ohkoshi, *Angew. Chem. Int. Ed.* **2015**, *54*, 5093-5097.

## Entry for the Table of Contents

## COMMUNICATION



Zongyao Zhang, Kunyi Zheng, Tianlong Xia, Lijin Xu, and Rui Cao\*

Page No. – Page No.

**Ni<sub>3</sub> vs Ni<sub>30</sub>. A Truncated Octahedron Metal-Organic Cage Constructed with [Ni<sub>5</sub>(CN)<sub>4</sub>]<sup>6+</sup> Squares and Tripodal Tris-tacn Ligands that are Large and Flexible**

**Unique coordination cage:** Trinickel complex of tripodal tris-tacn ligand assembles with cyanide ions, which are formed *in situ* via Ni-catalyzed C–CN bond cleavage of acetonitrile, to give a nano-sized Ni<sub>30</sub> cage under mild conditions. This molecular cage is unique because it represents a discrete truncated octahedron assembled with pentanuclear [Ni<sub>5</sub>(CN)<sub>4</sub>]<sup>6+</sup> squares and large and flexible triangular tris-tacn ligands, which has been scarcely observed for self-assembled metal-organic cages.